

# **Rock Mass Characterization and Conceptual Modeling of the Printzsköld Orebody of the Malmberget Mine, Sweden**

**Sraj Banda Umar<sup>1</sup>, Jonny Sjöberg<sup>2</sup> and Erling Nordlund<sup>3</sup>**

## **Abstract**

The LKAB Malmberget Mine is mined using sublevel caving. This mining method is cost-effective but results in successive caving of the host rock and mining-induced ground deformations. Consequently, re-locations of residential areas have been in progress in Malmberget ever since iron ore extraction on industrial scale commenced about a century ago. This study seeks to increase the understanding of the intrinsic characteristics of the rock mass governing deformation and caving activities. Rock mass characterizations were done in two selected orebodies — Printzsköld and Fabian. Two drill holes were drilled in each orebody from the surface. Geotechnical core logging was performed using the RMR system. Weakness zones were categorized to determine what role they played in the caving process. Point load testing was conducted for a sampling interval of about 5 m and selected uniaxial compressive strength tests were conducted to calibrate the point load index. Tunnel mapping was conducted in the hangingwall of the Printzsköld orebody. The finite element modeling code Phase2 was used for a sensitivity analysis of rock strength parameters and to study factors that may influence initiation of caving of the hangingwall.

**Keywords:** Mining-induced subsidence, rock strength, numerical analysis, weak zone characterization

## **1 Introduction**

### **1.1 Background**

The Malmberget mine is operated with large-scale sublevel caving. The mine comprises a total of 20 orebodies of which about 10 are in active production today. The mine is located in the municipality of Gällivare, see Figure 1 [1].

---

<sup>1</sup>Luleå University of Technology, Sweden.

<sup>2</sup>Itasca Consultants AB, Luleå, Sweden.

<sup>3</sup>Luleå University of Technology, Sweden.

Over the years, extraction from these orebodies has created varying subsidence problems on the ground surface, thus affecting residential areas and existing infrastructure. This subsidence is associated with the mining method which undermines the hangingwall causing instability and ground deformations. As mining progresses to deeper levels a larger subsidence area is created.

The subsidence zone on the surface is characterized by cracks, sinkholes and steps in many areas. Forecasting the subsidence processes is not straight-forward as it can be rapid or slow depending on the rock mass conditions, stress conditions, the mechanisms at work, etc. Moreover, several of the orebodies are non-daylighting, which makes reliable subsidence prognosis even more difficult.

Studies have been conducted [2, 3, 4, 5] in which many of these processes have been targeted and investigated in Malmberget mine; however, a deeper and detailed understanding of the subsidence processes is required. The present study was designed to improve the understanding of the subsidence mechanism of the Printzsköld orebody hangingwall.

The Printzsköld orebody is located in the central area of the Malmberget mine [2], and was chosen to be the case study orebody. This orebody was chosen for two reasons: (i) it is one of the more important orebodies in terms of future production volumes in Malmberget, and (ii) it is located partly beneath the central area of the Malmberget municipality with associated large impact, if caving to the ground surface developed. Since mining started in this orebody there has not been any subsidence on the ground surface, but a reliable prediction of future caving and associated ground deformations is lacking. This study comprised a rock mass characterization campaign and a conceptual numerical modeling of the Printzsköld orebody.

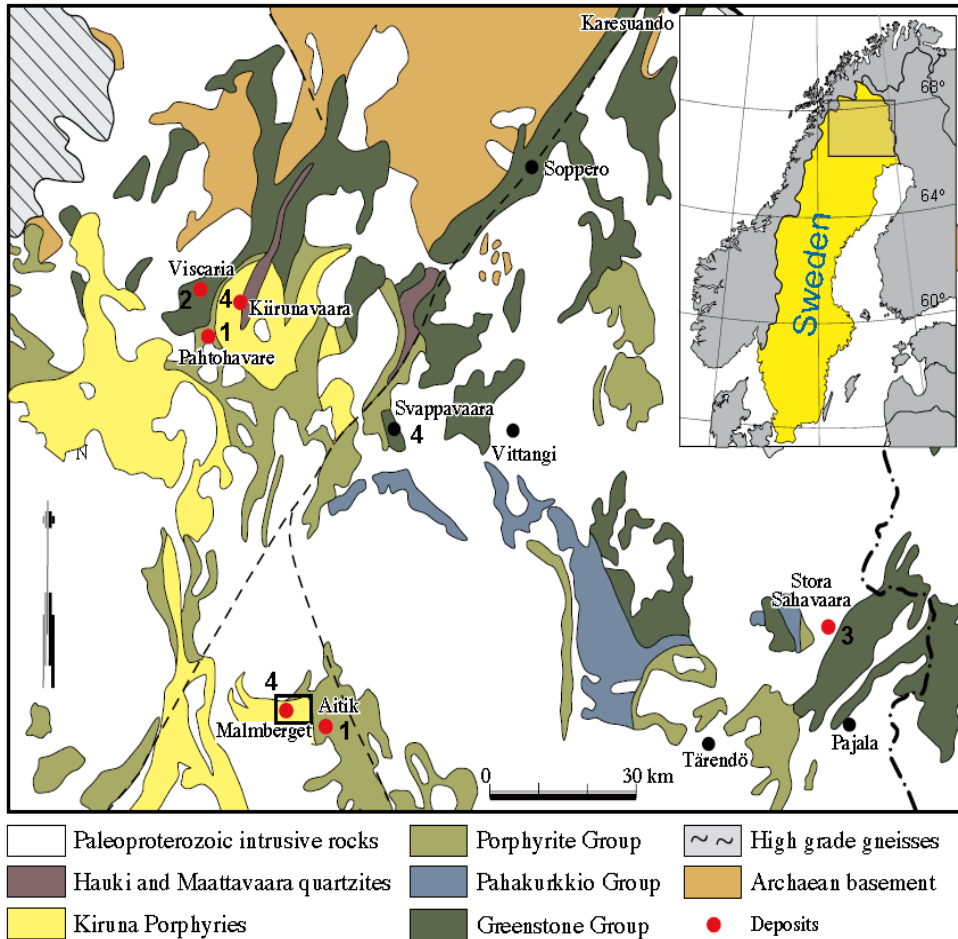


Figure 1: Geological map of the Northern Norrbotten Region (Sweden), (from [1])

## 2 Conceptual Model for Caving Analysis

### 2.1 Cave Mining

Laubscher [6] defines cave mining as all mining operations in which natural caving of the orebody is encouraged through undercutting [6]. It includes mining methods such as sublevel caving, block and panel caving, and inclined draw caving. These mining methods allow for the bulk beneficiation of large orebodies at a low cost [7]. Since their introduction in the early 20<sup>th</sup> century it has been very important for the mine operators to predict the cave propagation.

In [6], Laubscher also posits that this type of mining is the lowest-cost underground mining method as long as draw sizes are designed to equitable requirement for the material cavability. Among the 25 factors that Laubscher pointed out to be of primary consideration are surface subsidence and induced cave stresses [6].

For cave propagation to be successfully initiated a well-developed low-dip joint must be present which interacts with two steeply dipping joints to create a free falling block [8].

This assertion was earlier stated by [9] who suggested that when tangential stresses are low or tensile in nature free blocks may be able to slide on inclined discontinuities and fall by gravity in what is called gravity caving. These fallouts can also be augmented by the entire domains of weakness due to other factors such as shearing, weathering and dissolution. In [10] it is suggested that fallout conditions may develop when horizontal in situ stresses are low such as in those cases where slots and early mining have relieved the stresses or redistributed them away from the block [10].

Duplancic and Brady [11] developed a conceptual model for caving by analyzing the seismic responses in the vicinity of a cave. They found that a caving zone can be characterized by the zones shown in Figure 2.

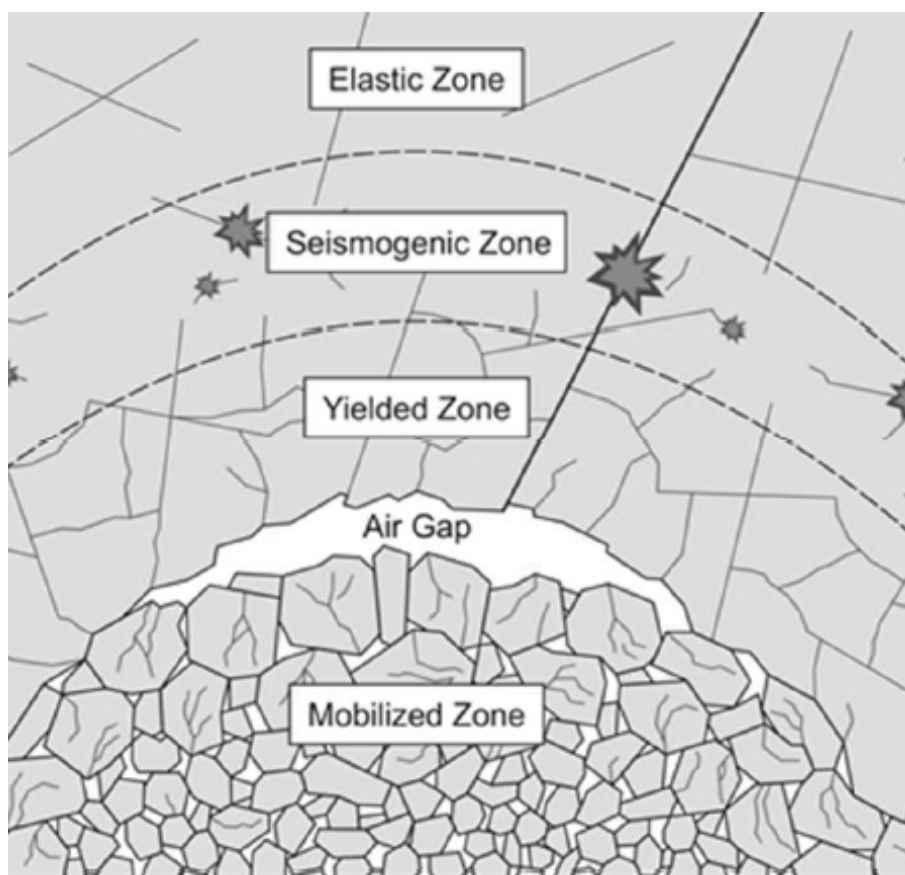


Figure 2: Conceptual model of the caving zone as proposed by [11].

The zones are described briefly here:

- i. Caved or mobilized zone  
This zone is made up of rocks that have been mobilized or broken. The material in this zone is considered cohesion less. This material also provides stability to the walls of the cave.
- ii. Air gap  
The extraction of the caved material affects the height of the air gap. This is the gap that is left at the back of the cave.
- iii. Zone of discontinuous deformation

In [11] this region was characterized as one that no longer provides support to the over-lying rock masses. Large scale movements of the rock mass have occurred in this region while no seismic activities are recorded.

iv. Seismogenic zone

In this region a seismic front occurs due to brittle failure of joints and their slip on joints. The behavior is attributed to the changing stress regime and the propagation of caving.

v. Elastic zone

This is the zone furthest from the cave. It is composed of intact rock mass and has an elastic behavior towards deformation. It is a region ahead of the seismic front.

Sublevel caving practiced at the Malmberget mine in the Printzsköld orebody fits into this model, since there is still a cap rock above the cave. Seismic monitoring in this orebody revealed trends of seismic activities in the hangingwall as well as the cap rock, which were consistent with the ones described in [11]. Also, the drill hole PRS01, drilled from the surface above the Printzsköld orebody in the hangingwall intercepted a void at a hole length of about 282 m, as shown in Figure 3.

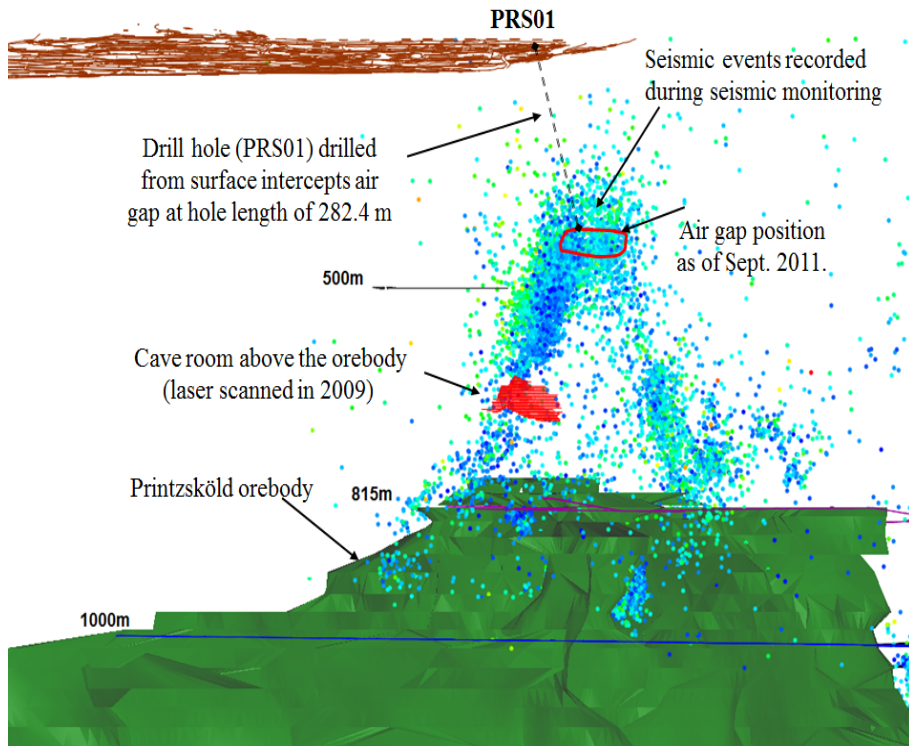


Figure 3: Seismic monitoring and drilling in the Printzsköld orebody conforming to the conceptual model of caving by [11] (courtesy of Malmberget Mine).

### **3 Rock Mass Characterization**

#### **3.1 Local Mine Geology**

The Malmberget deposit is a paleoproterozoic succession of greenstones, porphyries and clastic meta-sediments which are hosted by metavolcanics that have been intruded by pegmatites and granites [1] see Figure 1. The volcanic rocks have been transformed to sillimanite gneisses with quartz, muscovite, and local andalusite by the young granite intrusions. The iron ores are characterized by coarse magnetite and variable horizons of apatite with local sections rich in hematite. Generally, the border zones of the ore are characterized by skarn zones interpreted to be related to the formation of the ore [5]. Similar to many areas in Northern Sweden, the Malmberget deposit is characterized by NW-SE trending shear zones [5]. These zones are thought of as resulting from a complex geodynamic evolution which included repeated extensional and compressional tectonic regimes associated with magmatic and metamorphic events [12].

Two of the four diamond drill holes used, were placed in the hangingwall of the Printzsköld orebody with borehole numbers PRS01 and PRS02 and their respective azimuths indicated by the white arrows as shown in Figure 4. The two drill holes were drilled to about 280 m and 302 m respectively. The rock mass was mainly dry during drilling.

#### **3.2 Characterization of the Malmberget Mine.**

In the Malmberget Mine, many studies have been carried out aimed at characterizing the rock mass [3, 4]. Debras [3] tried to characterize the rock mass hosting the Printzsköld orebody, and offered a comprehensive petrologic and geologic description. Wänstedt, [4] carried out a rock mass characterization of the Malmberget rock using geophysical borehole logging [4]. He demonstrated the variations in rock mass properties, including rock mass strength, based on observations and deductions of rock densities from the geophysical electromagnetic methods.

However, the results of the previous work were not geotechnically useful as no explicit characterization of geotechnical parameters was done. The lack of geotechnical characterization of the Printzsköld and Fabian orebodies in Malmberget necessitated a more thorough rock mass characterization study.

#### **3.3 Data Collection and Results**

Geotechnical core logging and tunnel mapping was the major source of classification information for the various rock formations intercepted. Data was collected and processed in accordance with the Bieniawski (1989) Rock Mass Classification (RMR) system [13].

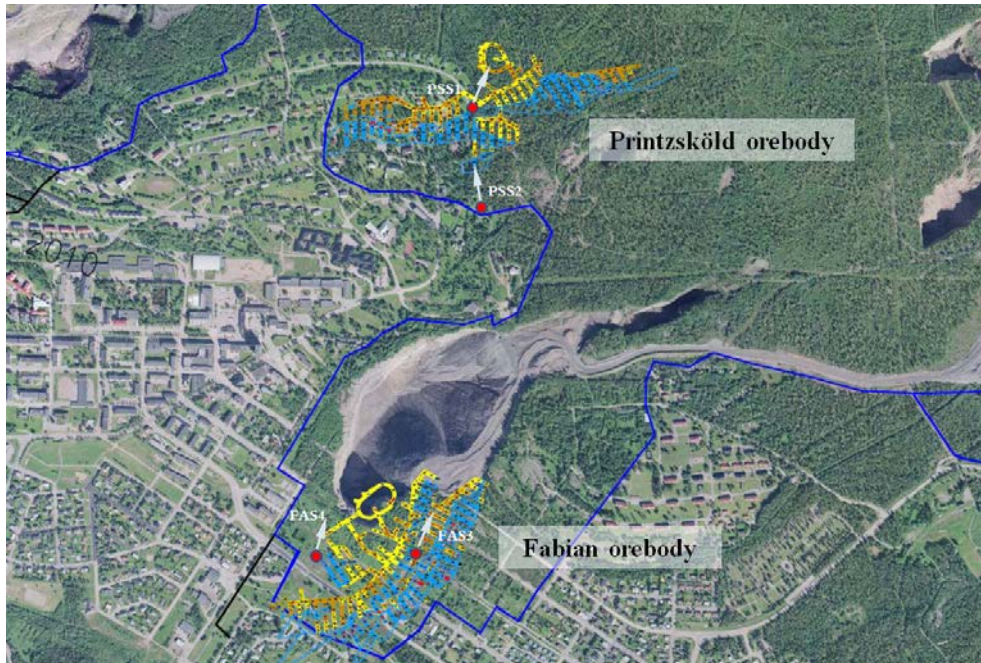


Figure 4: Drill hole locations for the Malmberget rock mass characterization. The orebody (magnetite in blue) and the footwall rock mass (Red Leptite in yellow, Red-Grey Leptite in brown) are shown as horizontal projections from the 945 m mine level (Courtesy of LKAB, Malmberget Mine, 2011).

Core logging consisted of physical inspection, measurement and observation of the diamond drill cores. This approach enabled the collection of information such as RQD length, natural breaks, rock mass formation and description, see example in Figure 5. Table 1 shows the rock formations intercepted in drilling and their descriptions

Table 1: Rock formations intercepted in the Printzsköld orebody

Rock formation	Abbrev	Description of rock
Red Leptite	RLE	Reddish-brown, medium to coarse grained feldspathic quartzite matrix, hard.
Grey Leptite	GLE	Grey medium grained, partly micaceous
Red-Grey Leptite	RGL	Pinkish grey, medium to coarse grained, hard, micaceous in many places
Magnetite	MGN	Greenish grey, dark patches, medium grained, micaceous.
Skarn	SKN	Dark, green, coarse grained.



Figure 5: Example of rock core from the Printzsköld orebody drill holes.

Tunnel mapping was undertaken in the Printzsköld orebody on 970 and 945 m levels see Figure 6. Other characteristics investigated were the geological strength index (GSI) [14], estimated from the rock mass characteristics in the field; joint orientations, and general rock mass descriptions. Table 2 shows the GSI values obtained from tunnel mapping of the 945 and 970 m levels in the Printzsköld orebody.

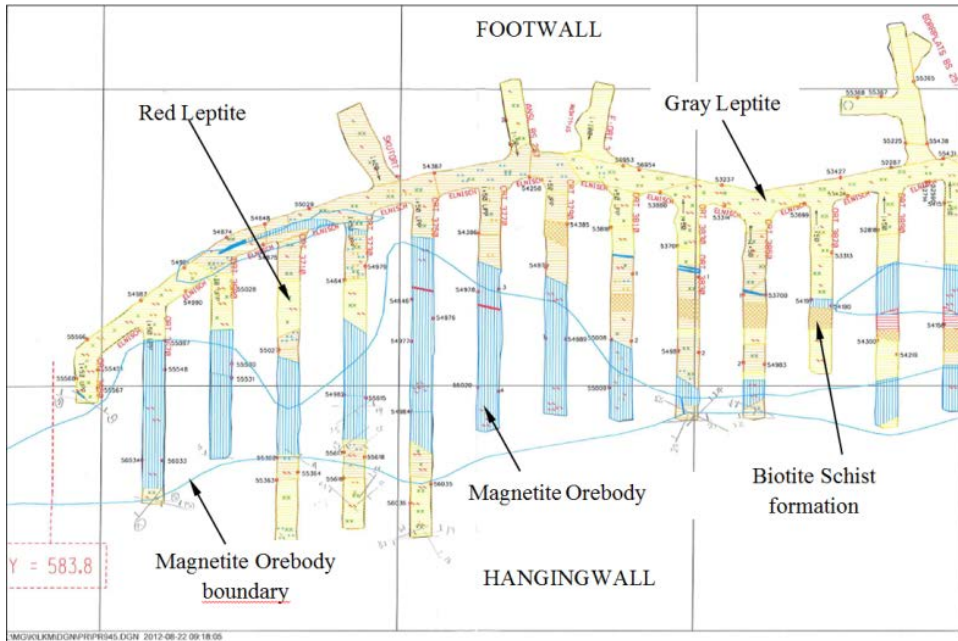


Figure 6: The 945 m level in the Printzsköld orebody in which underground mapping was carried out. (Courtesy of LKAB, Malmberget Mine, 2012)

Table 2: GSI values as obtained from mapping the 945 and 970 m levels in the Printzsköld orebody

Rock Formation	GS I	Conditio ns	Comment
Red Leptite (RLE)	68	GOOD	Blocky, slightly weathered iron stained
Grey Leptite (GLE)	64	GOOD	Blocky, slightly weathered joints, iron stained.
Red-Grey Leptite (RGL)	40	FAIR	moderately weathered and altered surfaces
Magnetite (MGN)	65	GOOD	rough and slightly weathered highly weathered surfaces and slicken sides
BiotiteSchists (BIO)	20	POOR	joints, seamy

### 3.4 Point Load Strength Testing

Sampling of rock cores for intact rock strength was conducted at an interval of 5 m along the borehole. Samples were prepared for axial as well as diametral point load strength testing as described in [15]. Care was taken to apply the force at the rate of 10-60 seconds to the break of the sample in either direction. Laboratory direct uniaxial compressive strength test results from ten samples were used to calibrate the point load index as shown in Figure 7, which was found to be 21 MPa. The resulting intact rock strengths derived directly from the point load testing were subsequently used in the determination of the RMR values for this area.

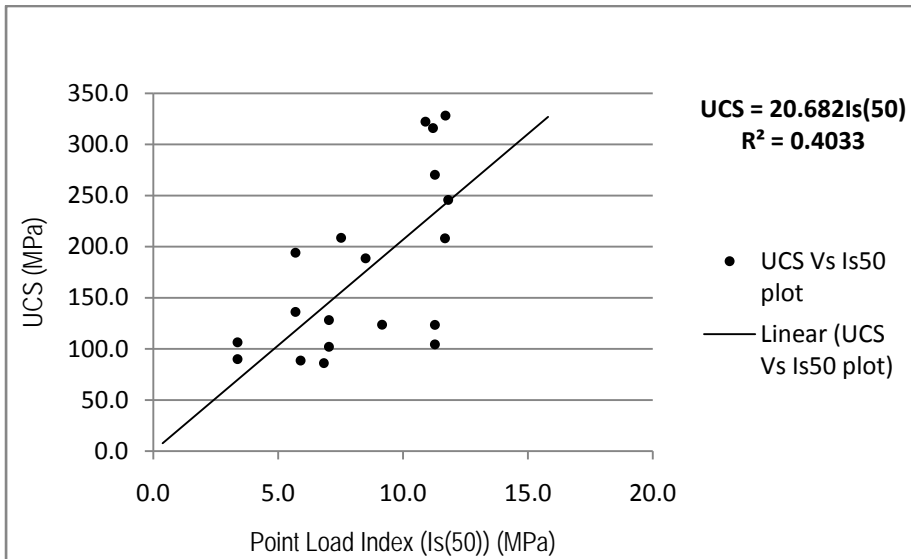


Figure 7: Point Load Index Calibration using Direct Uniaxial Compressive Strength (UCS) test results.

Intact rock strength results showed that most of the rock mass is highly competent and hard. Table 3 shows UCS strength results for the Malmberget area for each rock formation intercepted. The disparities in minimum and maximum values in these values were due to various weak zones.

Table 3: Uniaxial compressive strength values for the Printzsköld orebody, Malmberget.

Rock Formation	UCS* [MPa]		
	Max	Min	Average
Red Leptite (RLE)	302	60	184
Grey Leptite (GLE)	242	90	149
Red-Grey Leptite (RGL)	256	120	176
Skarn (SKN)	170	74	127
Magnetite (MGN)	182	71	127

\* values from point load tests

### 3.5 Rock Strength Isotropy

The rock units around the Printzsköld orebody showed considerable strength isotropy. The axial-to-diametral strength ratio is shown in Figure 8 (a and b).

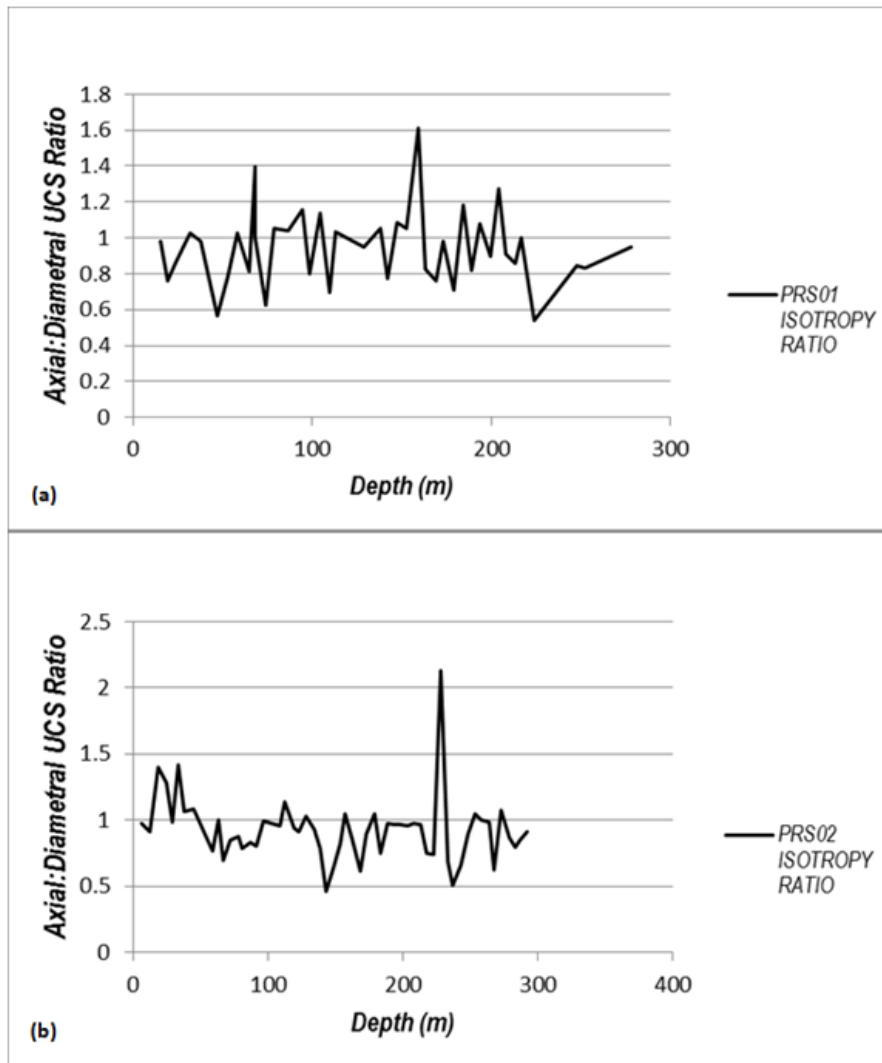


Figure 8: Intact rock strength isotropy ratio in the Printzsköld orebody.

With the exception of a few outliers, the majority of the test data indicated isotropy ratios of between 0.6 and 1.1 for the Printzsköld orebody, see also Figure 9. This suggests that this is a fairly isotropic rock with respect to strength. Anisotropy was found to be characteristic of biotite schist zones and areas generally categorized as weak zones as observed from core logging and tunnel mapping.

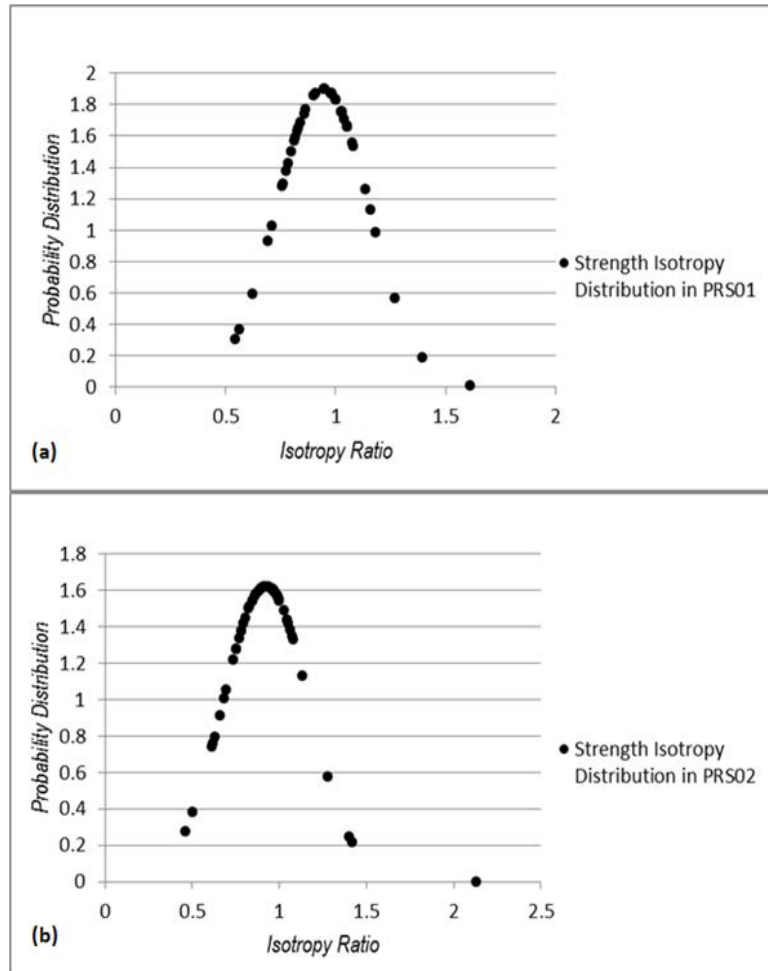


Figure 9: Normal distribution of the intact rock strength isotropy in the Printzsköld orebody, as inferred from point load tests.

### 3.6 Rock Mass Rating (RMR) and Rock Quality Designation (RQD)

Tables 4 and 5 show value ranges for rock quality designation (RQD) [16]; and rock mass ratings (RMR) [13] for the Printzsköld orebody rock units. Rock mass rating showed that most of the rock mass was classified as good rock

Table 4: RQD values for the Printzsköld orebody, Malmberget mine.

Rock Formation	RQD%		
	Max	Min	Average
RLE	97	24	71
GLE	94	28	65
RGL	93	46	69
SKN	90	65	85
MGN	79	68	73

Table 5: RMR for the Printzsköld orebody, Malmberget mine.

Rock Formation	RMR			Class (based on Average)
	Max	Min	Average	
RLE	78	54	66	II
GLE	69	53	63	II
RGL	70	60	67	II
SKN	67	65	66	II
MGN	67	62	65	II

The distribution of RQD and RMR has been graphically presented for boreholes PRS01 and PRS02 in Figure 10. The RMR in the orebody hangingwall fluctuates between 65 and 75, with many rock formations reaching a maximum of 80.

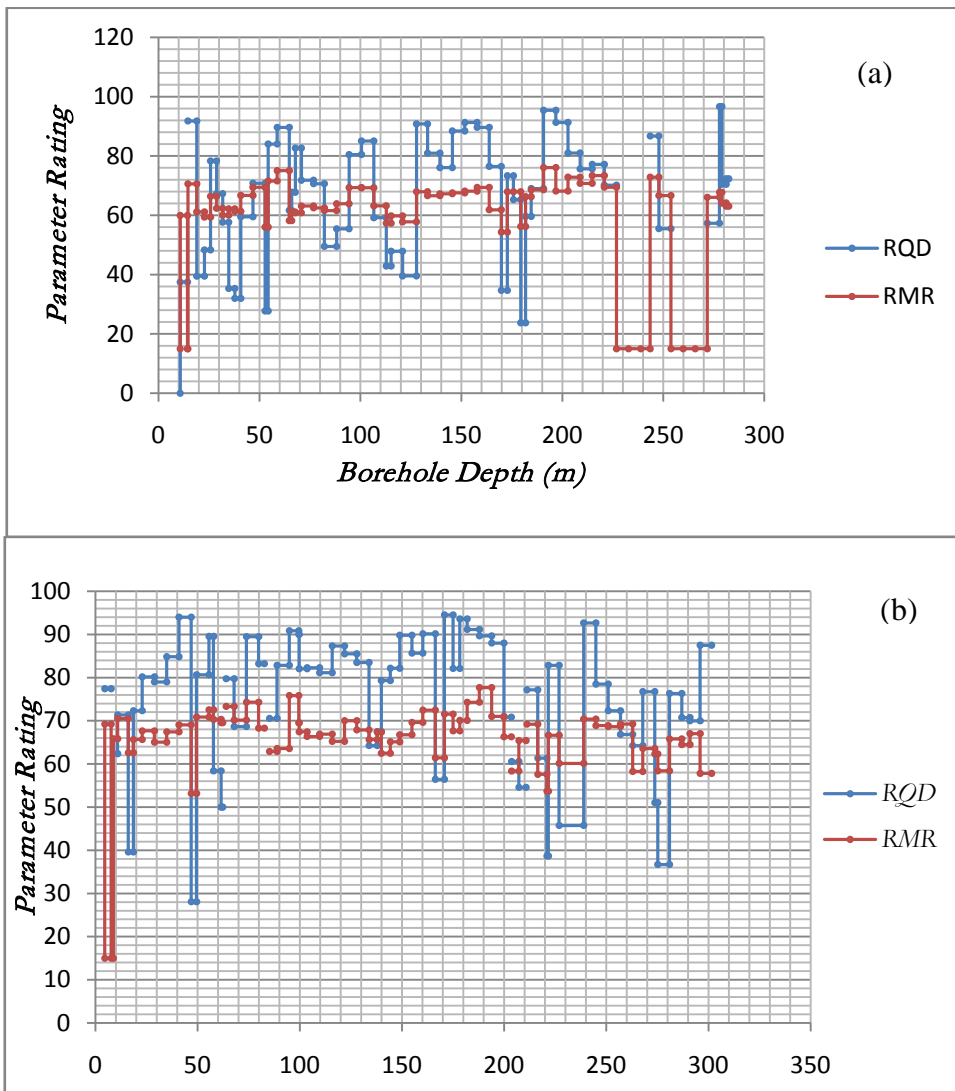


Figure 10: RMR and RQD distribution for the Printzsköld area. Both boreholes PRS01 (a) and PRS02 (b) showed similar value ranges.

### 3.7 Joint Descriptions

Three main joint sets were found in the hangingwall of the Printzsköld orebody. The joint conditions are summarized as follows:

- Moderately weathered, predominantly rough planar joint, hard infilling, some soft infill found in some joints.
- Joint spacing of 10 to 50 cm.
- Predominantly hard kaolinitic in fills.
- Joint orientations (dip/dip-direction) were: (i) 27°/346°, (ii) 13°/097°, and (iii) 72°/173°

### 3.8 Weak Zones

Weak zones were encountered in the Printzsköld hangingwall. These zones had properties different from the host rock and as such they needed to be systematically evaluated to determine their effect on overall stability of the rock mass. It was found that the weak zones had an impact on the rock strength isotropy in the Printzsköld orebody as seen from the distorted ratio plots for isotropy comparisons in Figure 6. Weak zones were divided into two categories: (i) highly fractured zones, and (ii) weathered/low strength zones.

The highly fractured zones comprised rocks characterized by many fractures and they showed diskings in some places due to stress concentrations. These were commonly observed in rock formations such as red leptite (RLE) in the hangingwall.

The weathered low strength zones were made up of rocks that exhibited weaknesses due to material types, alteration and weathering. The material weaknesses were characteristic of all biotite zones found mostly in grey leptites as well as marking the contacts with the orebody magnetite (MGN). Figure 11 shows weak zones intercepted by each drill hole and their distributions.

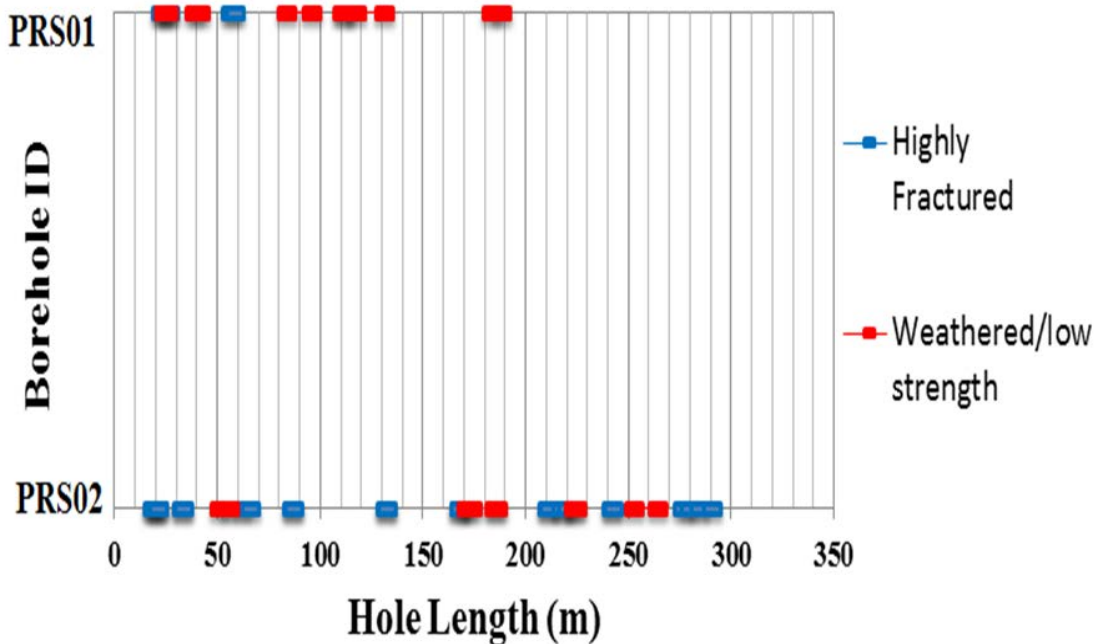


Figure 11: Weak zone intervals presented for each borehole

## 4 Numerical Modeling of the Printzsköld Orebody

### 4.1 Approach

The objective of the conceptual modeling of the Printzsköld orebody was to assess the sensitivity of strength parameters. The aim was also to provide insight into possible failure mechanism(s) of the hangingwall.

*Phase2*, a Finite Element Modeling (FEM) program from *Rocscience Inc.* [17] was used to analyze the stress re-distribution of the Printzsköld orebody hangingwall. The Printzsköld orebody has a complex geometry which require some geometrical simplifications. In this initial work, only a two-dimensional analysis was conducted, in which a vertical cross-section of the orebody and hangingwall was modeled, see Figure 12. This rather severe simplification was judged acceptable to study, conceptually, stress distribution and possible failure mechanisms of the hangingwall. Three-dimensional modeling, enabling including the plunge of the orebody, is obviously required in future work. However, the vertical cross-section perpendicular to the orebody strike was believed to, at least in some aspects, be justified in a two-dimensional model, see Figure 12.

Caving was not explicitly simulated. Rather, the caved rock was simulated as a void, starting from the current situation, in which caving has progressed to about 300 m below the ground surface. The conceptual model was aimed at investigating the stability of the existing cave and factors that may trigger additional cave growth. The hangingwall response in this case was analyzed using both elastic and plastic material models.

### 4.2 Model Set-Up

Mining of the Printzsköld orebody started at the 780 m level. With continued mining toward depth, the cap rock caved and the cave advanced to the current depth of about 300 m below ground surface as of 2012, as shown in Figure 13. This mining and cave development has not been simulated in this model. Rather, simulation started with the extraction of 920 m level (mined in 2011). Sublevel heights in the mine are 25 m, but were slightly simplified in the model so that each mining level was set at 25 to 30 m from the sublevel below, and mining was simulated down to the 1052 m level (a total of six mining stages).

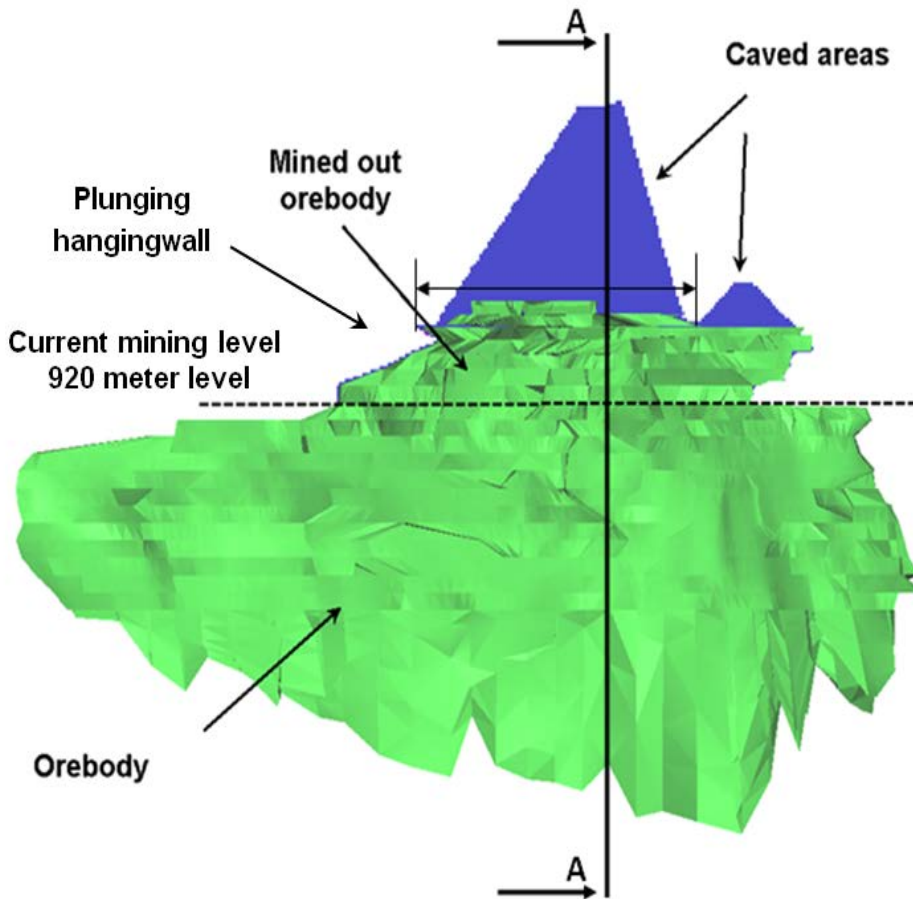


Figure 12: 3D model of the Printzsköld orebody. Section line A-A indicates where the cross-section of the numerical model has been taken from.

The model length was set to 3.2 km and the depth to 1.7 km, to accommodate the entire Printzsköld orebody, both the caved and previously mined parts as well as the un-mined delineated orebody. The model size was chosen to minimize possible boundary effects. A query line for interpretation was offset at about 10 – 15 m from the hangingwall boundary, see Figure 13.

### 4.3 Mechanical Properties

The elastic constants used in this model were derived from [20] and they were Young's modulus  $E = 70$  GPa and Poisson's ratio  $\nu = 0.27$  for the host rock mass (both footwall and hangingwall). For the orebody the values were set at 65 GPa and 0.25 respectively. The density of the host rock was set at  $2700 \text{ kg/m}^3$  and that for the orebody was set to  $4700 \text{ kg/m}^3$ .

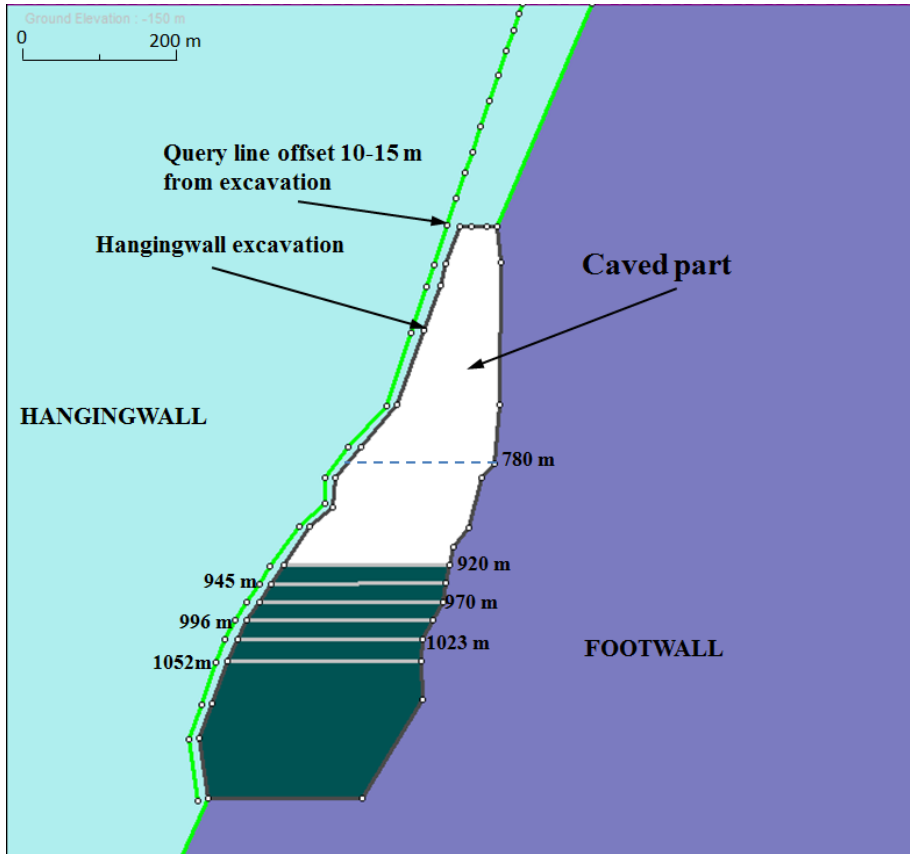


Figure 13: Cross-section of the Printzsköld orebody in the Malmberget mine.

The rock strength parameters were also taken from [18]. Table 6 shows the strength parameter values in previous studies for the Malmberget area.

Table 6: Typical strength parameters for the Malmberget Mine. (from [18])

Unit	c [MPa]	$\phi$ [°]	$\sigma_{im}$ [MPa]
Global, mine-scale model			
Hangingwall	5.18	50.7	0.71
Orebody	4.81	50.7	0.48
Footwall	6.67	52.9	1.30
Local, drift-scale model			
Footwall — Low	4.55	50.3	0.37
Footwall — High	6.67	54.8	1.04

The joint strength parameters were obtained from [19] as follows:

- Normal joint stiffness: 110 GPa/m.
- Shear joint stiffness: 9 GPa/m.
- Joint friction angle: 35°.
- Joint cohesion: 0 MPa.

The selected input parameters for the plastic models are shown in Table 7. This model was run using an elastic-perfectly plastic Mohr-Coulomb material model.

Table 7: Strength parameters used for the plastic models

Area	Strength parameter	Peak value	Residualvalue
Hangingwall	c [MPa]	5.15	5.18
	$\phi$ [°]	50.7	50.7
	$\sigma_{tm}$ [MPa]	0.71	0.71
Orebody	c [MPa]	4.81	4.81
	$\phi$ [°]	50.7	50.7
	$\sigma_{tm}$ [MPa]	0.48	0.48
Footwall	c [MPa]	6.67	6.67
	$\phi$ [°]	52.9	52.9
	$\sigma_{tm}$ [MPa]	1.3	1.3

c = cohesion;  $\phi$  = internal friction angle;  $\sigma_{tm}$  = tensile strength

The sensitivity analysis performed using the elastic model was based on the estimated input strength values obtained above. Parameters were varied over the ranges according to Table 8.

Table 8: Ranges of strength parameters used in the models

Strength Parameter	Value			
c [MPa]	4	6	8	10
$\phi$ [°]	30	40	60	
$\sigma_{tm}$ [MPa]	0	0.5	1	1.5

#### 4.4 In-Situ Stresses

The rock stresses used in this model were derived from those used in [18], which comprised a numerical stress calibration against conducted measurements. The vertical stresses were considered to equal the pressure of overburden material at a given depth. The principal horizontal stresses were given by the equations below [19]:

$$\sigma_H = 0.0356z \quad (1)$$

$$\sigma_h = 0.0172z \quad (2)$$

where  $z$  is the vertical depth below ground surface in m, and  $\sigma_H$  has an orientation of 130.6° clockwise from local north.

#### 4.5 Model Results

Linear elastic continuum models were first analyzed and the resulting stress distribution studied. Subsequently, the strength factors (essentially factors of safety) for various combinations of strength parameters were calculated. Variations in cohesion, internal friction angle and tensile strength showed that the rock mass behavior was most sensitive to changes in the cohesion.

The distribution of strength factors in the elastic models provided an indication for low or high values of tensile or compressive stresses. Strength factors that reached zero were tensile stressed regions. In the plastic analysis it was possible to show the yielding in these zones and identify possible failure mechanisms in the hangingwall.

The elastic models showed that there were extensive areas of low stresses in the hangingwall as shown in Figures 14 and 15. A zone of relatively high compressive stresses was observed in the cap rock. However, low stresses were observed close to the ground surface as shown on point X.

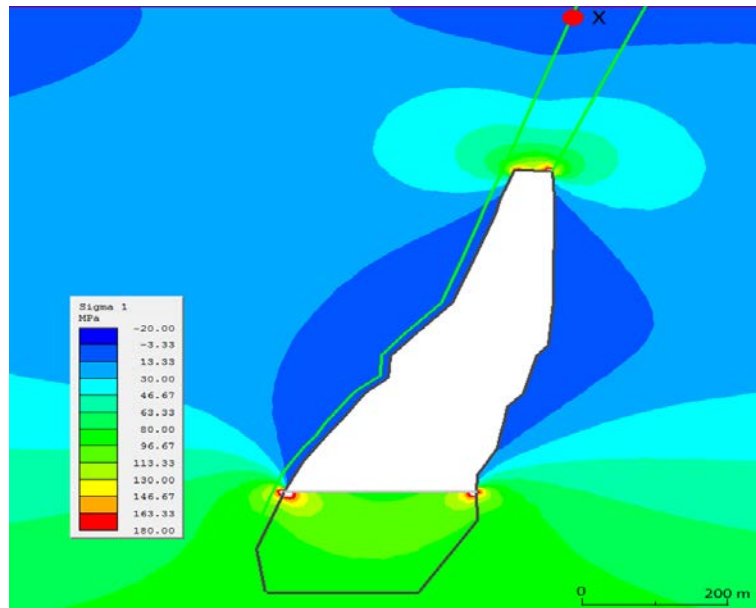


Figure 14: Distribution of  $\sigma_1$  after mining the 1052 level.

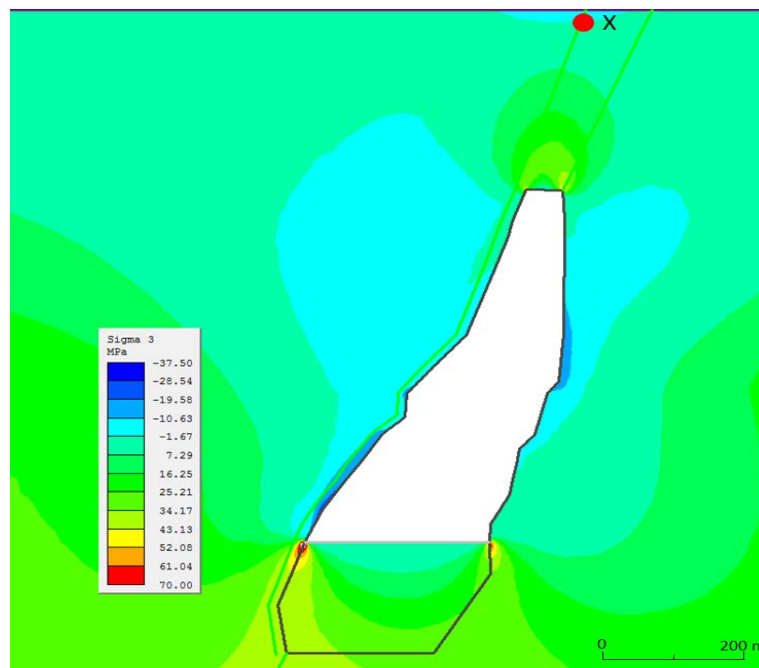


Figure 15: Distribution of stress  $\sigma_3$  for mining level 1052 m.

On the query line, the value of strength factor can be seen at point X for both cohesion and internal friction angle variations see Figures 16 and 17. The strength factors have high values because in these areas, the stresses are low, but because of low confinement, the strength is also low. In relative terms (strength factor defined as a ratio) the strength factor may be high, but even a slight increase in stress may cause the strength factor to drop significantly. In essence this can give an implication of adequate factor of safety in as far as failure is concerned. As will be shown in the plastic model this whole region is susceptible to failure.

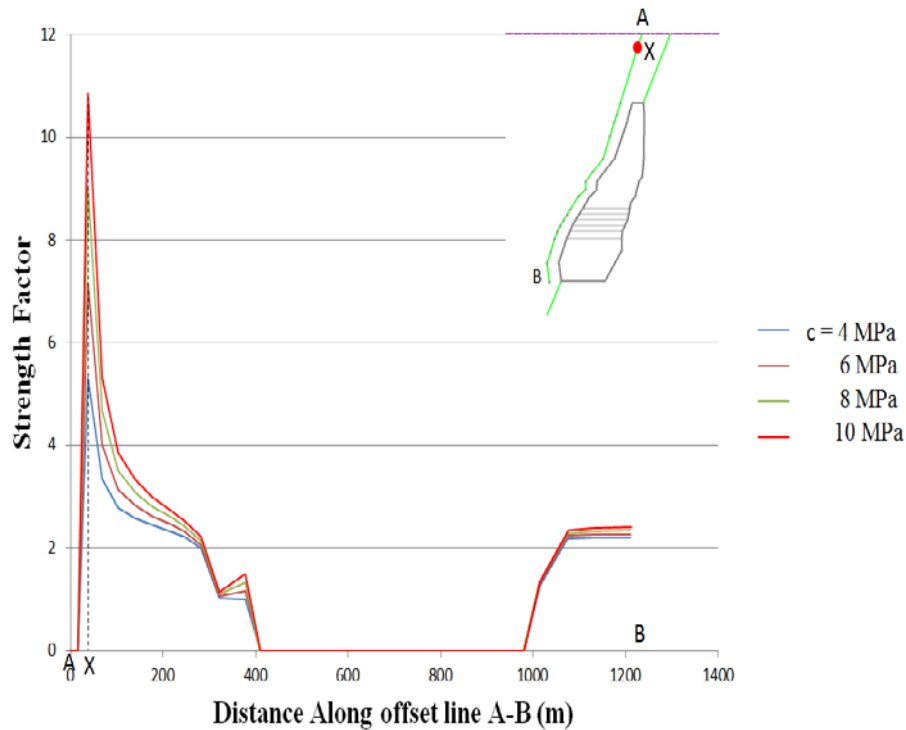


Figure 16: Strength factor associated with variations in cohesion on the 10-15 m offset query line

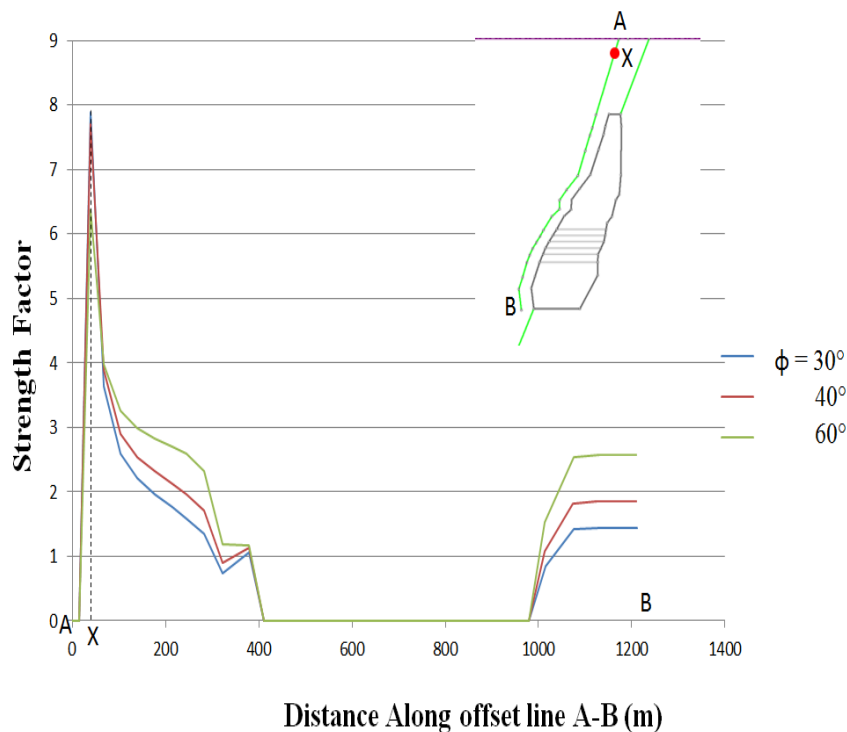


Figure 17: Strength factor variations on 10-15 m offset query line due to variations in internal friction angle.

A ubiquitous joint post analysis investigation for joint orientations (anti-clockwise from the positive x-axis) of  $-72^\circ$  and  $27^\circ$  (defined anti-clockwise from the positive x-axis) was performed. For the  $72^\circ$  joint set the zone of tensile strength in the hangingwall remained relatively smaller. For the  $27^\circ$  joint set the strength factors changed significantly and the indicated zone of tensile failure increased outwardly.

#### 4.6 Yielding and Failure Mechanisms

A plastic model was used to determine possible yielding and failure mechanisms for the hangingwall. Figure 18 shows yielded elements of the plastic model indicating areas of shear and tensile stresses. The zones of yielding correlate, qualitatively, with the regions observed earlier in the elastic models as having low strength factors. In this model the entire hangingwall showed tensile yielding while a mixture of shear and tensile yielding was observed in the back of the caved room. Shear failure regions were also observed towards the bottom of the caved area.

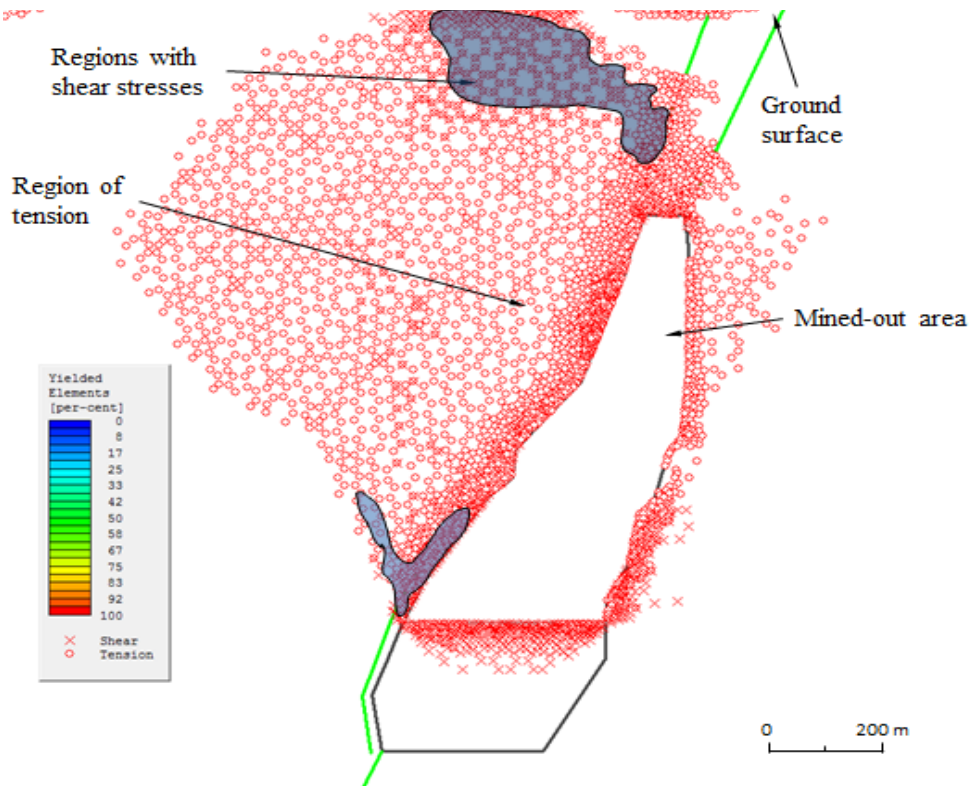


Figure 18: Yielded elements of the hangingwall of the Printzsköld orebody at the mining level of 1052 m.

The results also showed that as the mining depth increased the boundary of the yielded zone in the hangingwall increased progressively. Figures 19 through 21 show progressive yielding with deepened mining from 920 to 1052 m.

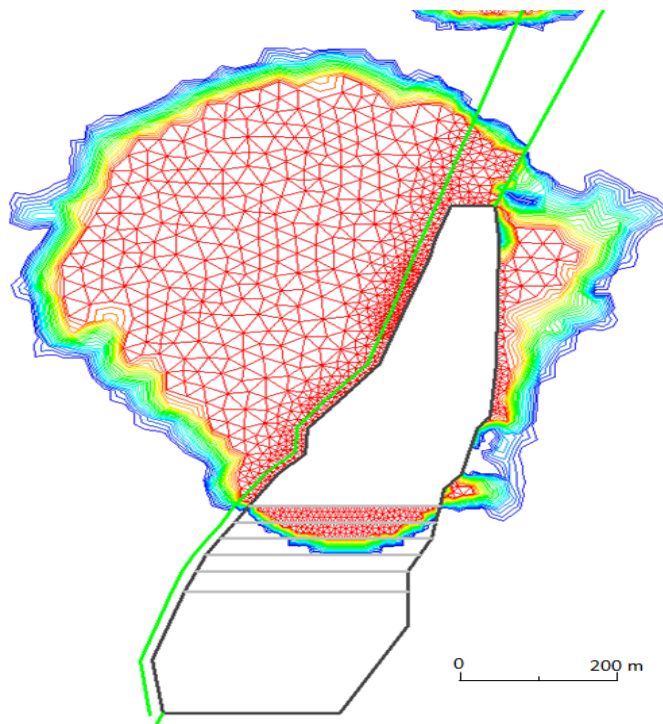


Figure 19: Yielding for mining of the 920 m level in the Printzsköld orebody.

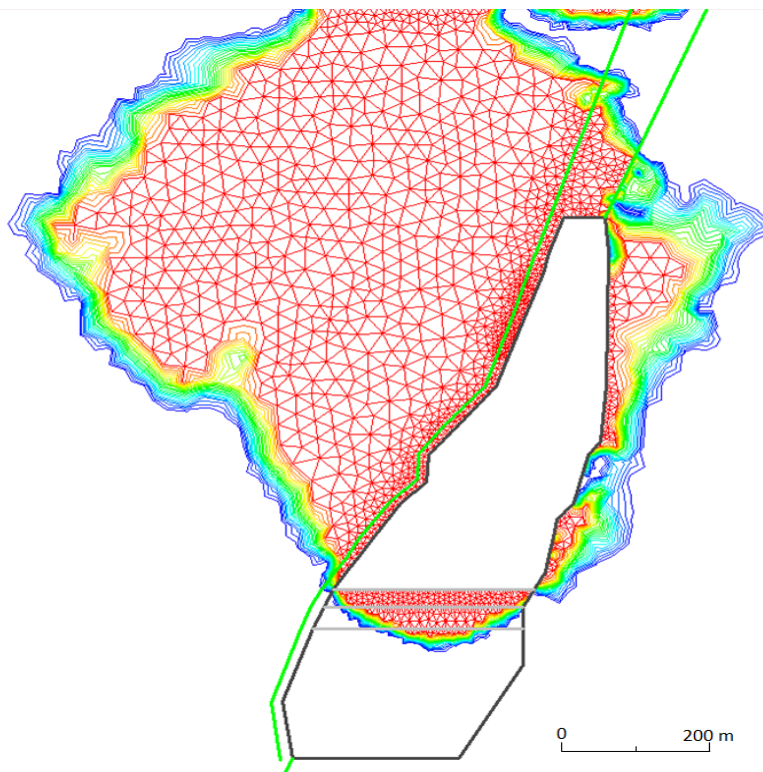


Figure 20: Yielding for mining of the 996 m level in the Printzsköld orebody.

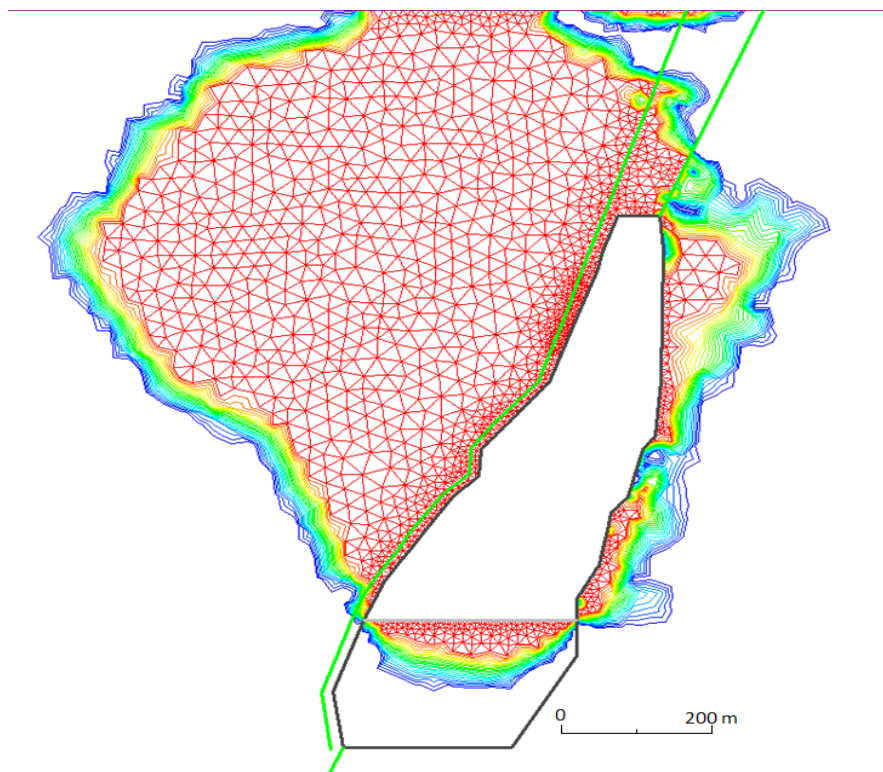


Figure 21: Yielding for mining of the 1052 m level in the Printzsköld orebody.

## 5 Discussion

The Printzsköld orebody is hosted within a relatively strong and competent rock mass. Rock core logged from this orebody showed five main rock formations: Red Leptite, Grey-Red Leptite, Grey Leptite, Magnetite (orebody formation) and Skarn. The length of the drill holes did not enable granite rock formation present in this region to be core drilled for examination; however, its presence has been inferred from other studies such as [2]. There was also biotite schist zones observed in the contacts between Grey Leptite and Magnetite. These biotite zones were characterized as part of the weak zones of the Printzsköld orebody.

The average RMR range for the competent rock masses was 63 to 67. Individual rock formations exhibited rock mass ratings as high as 80. Biotite schist zones present a geotechnical challenge in this orebody due to their weakness. Tunnel mapping showed that most of the areas containing biotiteschists had an effect of lowering the RMR to as low as 30, while the GSI was found to be reduced to around 20.

The rock mass also exhibited a relatively high strength isotropy in all rock masses. The loss of isotropy was observed in parts characterized as weak zones. It was not possible to fully describe the weak zones in the Printzsköld orebody as data obtained from the two diamond drill holes was too far apart to allow any correlation.

The sensitivities of the hangingwall and cap rock to variations in rock mass strength parameters have been studied. The strength factor was most sensitive to variations in cohesion.

The plastic model showed a yielding in the hangingwall and a major part of the hangingwall was exposed to tensile stresses, giving us a tensile failure mechanism of the rock mass into the mined out area. It also indicated that a likely progressive failure under the mechanisms given above could ensue as the depth of mining increases.

While this model offers a starting point for the evaluation of stress redistribution in the hangingwall in the cross section of the Printzsköld orebody, it does not fully capture an accurate description of stresses and failure distribution since failure is taking place in a three dimensional system.

As a preliminary analysis of this orebody, fairly large simplifications have been employed to make the model as simple and understandable as possible. Some challenges were met pertaining to the numerical code (*Phase2*) output of strength factors in the post analysis interpretation. High values of strength factors were found in areas with very low confining stresses. These values do not necessarily reflect stability but rather that the strength was also low. The high values of strength factor could be misinterpreted as safe areas.

## 6 Conclusions and Recommendations

From this study the following conclusion can be drawn:

- The results of the rock mass characterization showed that the rock mass strength in the Printzsköld area is generally high and competent.
- The averaged RMR across the rock formations ranged between 63 and 67, while the RQD had an average value in the interval of 71 to 85 %. The rock mass also had a GSI range of 60 to 75. GSI values were found to be very low in areas characterized by biotite schist.
- Numerical elastic models of the hangingwall of the Printzsköld orebody showed that the sensitivity of the hangingwall behavior was strongest for variations in cohesion.

The following recommendations are given:

- It is recommended that more joint orientation mapping be carried out in the lower levels of the Printzsköld orebody.
- More geotechnical drilling is required to ascertain rock mass geotechnical parameters for the lower levels of the Printzsköld orebody area which can be compared to those of upper levels obtained in this study.
- Drilling will also provide more information in the analysis of weak zones, their spatial distributions and their categorizations.
- A three dimensional model approach needs to be undertaken to account for the whole orebody geometry and stress interactions.

**ACKNOWLEDGEMENTS:** The authors would like to thank LoussavaaraKirunavaara AB (LKAB), The HjalmarLundbohm Research Centre (HLRC) and the Centre for Applied Mining and Metallurgy (CAMM) at LTU for funding this research. Special thanks go to Tomas Savilahti at the LKAB Malmberget Mine, for his continuous assistance for the smooth running of the study. Thanks also go to the entire research group members: Linda Jacobsson, Jimmy Töyrä, Fredrik Ersholm and Joel Andersson, all of LKAB, for their guidance, assistance and support during this research.

## References

- [1] Martinsson, O. and K. E. Hansson. 2004. Day seven field guide, Apatite Iron ores in the Kiruna Area.
- [2] Wettainen, T. 2010. Analys och prognostisering av uppblockning i Printzsköld. *Licentiate Thesis. Luleå, Sweden: Luleå University of Technology*. ISSN: 1402-1617.
- [3] Debras, C. 2010. Petrology, geochemistry and structure of the host rock for the Printzsköld ore body in the Malmberget deposit. *Master Thesis. Luleå: Luleå university of Technology*; ISSN: 1653-0187.
- [4] Wänstedt, S. 1991. Geophysical borehole logging in Malmberget. *Technical Report. Luleå University of Technology*; 14T.
- [5] Romer, R.L. 1996. U-Pb system of stilbite-bearing low-temperature mineral assemblages from the Malmberget iron ore, Northern Sweden. *GeochimCosmochimActa* 6; 60(11):1951-1961.
- [6] Laubscher, D.H. 1994. Cave mining - the state of the art. *J South Afr Inst Min Metall*; **94**(10):279-293.
- [7] Sainsbury, B.L., D.P. Sainsbury, and M.E. Pierce. 2011. A historical review of the development of numerical cave propagation simulations. *Proceedings of the 2nd International FLAC/DEM Symposium in Numerical Modeling*; Feb 14-16.
- [8] Kendorski, F.S. 1979. Cavability of ore deposits: *Min Engng*, V30, N6, June 1978, P628–631. *International Journal of Rock Mechanics and Mining Sciences & Geomechanics Abstracts*. 2; **16**(1):A8.
- [9] Mahtab, M.A., D.D. Bolstad, and F.S. Kendorski. 1973. Analysis of the geometry of fractures in San Manuel Copper Mine, Arizona; 7715.
- [10] Brown, E.T. 2003. Block Caving Geomechanics, The International Caving Study Stage 1 1997-2001, Australia: *JKMRC*, University of Queensland.
- [11] Duplancic, P. and B.H. Brady. 1999. Characterization of caving mechanisms by analysis of seismicity and rock stress. *9th International Congress on Rock Mechanics Characterization of caving mechanisms by analysis of seismicity and rock stress*. A.A. Balkema.
- [12] Skiöld, T. 1988. Implications of new U-Pb zircon chronology to early proterozoic crustal accretion in northern Sweden. *Precambrian Res* 2; **38**(2):147-164.
- [13] Bieniawski, Z.T. Engineering Rock Mass Classifications, **251**. *New York* (1989), *John Wiley & Sons*.
- [14] Hoek, E., P. Marinos, and M. Benissi. Applicability of the geological strength index (GSI) classification for very weak and sheared rock masses. The case of the Athens Schist Formation. *Bulletin of Engineering Geology and the Environment*; **57**(2), (1998), 151-160.
- [15] Broch, E. and J.A. Franklin The point-load strength test. *International Journal of Rock Mechanics and Mining Sciences & Geomechanics Abstracts* (1972), 11; **9**(6):669-676.
- [16] Deere, D.U. and R. D. Miller. Engineering classification and index properties for intact rock, *AFWL-TR* (1966), **65**.116.
- [17] Rocscience Inc. Phase2 Version 6.028 - Finite Element Analysis for Excavations and Slopes. *www.rocscience.com*, Toronto, Ontario, Canada.2008.
- [18] Sjöberg, J. Three-Dimensional Unit Stress Tensor Modeling of Complex Orebody Geometry. *American Rock Mechanics Association (ARMA)*.2008.

- [19] Malmgren L., and E. Nordlund. Interaction of shotcrete with rock and rock bolts—A numerical study. *Int J Rock Mech Min Sci*, **6**;45(4), (2008), 538-553